3. *Zinc.* A small electric crucible which contained small pieces of Zn metal was introduced in the discharge tube. N-heptane vapor sustained the discharge, while the zinc was vaporized by electric heating. Doublets and mass differences obtained were as follows:

Doublets	Number of doublets measured	Mass differences ($\times 10^{-4}$ M.U.)
$C^{12}_5H^1_{14}-Zn^{64}$	13	982.3±6.4
$C^{12}_5H^1_{16}-Zn^{66}$	17	1213.8±3.9
$C^{12}_6H^1_7-Zn^{67}$	8	1280.1±6.3
$C^{12}_6H^1_8-Zn^{68}$	8	1355.5±6.3
$C^{12}_6H^1_{10}-Zn^{70}$	3	1346.0±16

4. *Bromine.* Discharge was operated through the mixture of normal heptane vapor and sublimated vapor of titanium tetrabromide crystals. Since doublets could not be obtained in this case, dispersion curves were drawn by the least square method with five hydrocarbon lines, $C^{12}_3H^1_2$, $C^{12}_3H^1_3$, $C^{12}_3H^1_4$, $C^{12}_3H^1_5$, and $C^{12}_3H^1_6$, which covered the doubly ionized region of Br. From these dispersion curves and the mass $H^1=1.0081$, the following mass differences were obtained:

Mass differences	Number measured
$\frac{1}{3}Br^{79}-C^{12}_3H^1_3=0.43618\pm2.3\times10^{-4}$	11
$\frac{1}{3}Br^{81}-C^{12}_3H^1_4=0.42700\pm1.6\times10^{-4}$	11

From these above results of the mass differences and the value $H^1=1.008131\pm0.033\times10^{-4}$, $C^{12}=12.003871\pm0.33\times10^{-4}$,[1] the isotopic weights of all these isotopes were calculated. The isotopic weights, the packing fractions, and the binding energies which were calculated from the mass of hydrogen (1.008131) and neutron (1.008945) are summarized in Table I. In the last column are given theoretical binding energies, calculated from Nakabayashi's formula of the binding energy,[2]

$$E=-15.2A+20(N-Z)^2/A+14.6A^{\frac{2}{3}}+0.62Z^2A^{-\frac{1}{3}}(10^{-3}\text{ M.U.})$$

here, A is mass number, Z is number of protons, and N is number of neutrons.

The packing fraction curves were drawn in this region by using these results and the values of Ti[3] and Ni[4] reported in our previous paper.

It is seen from these curves (Fig. 1) that the packing fraction of the isotopes of the same elements differ considerably from each other. It is worth noticing especially that in the four pairs of isobars, $Ti^{50}-Cr^{50}$, $Cr^{54}-Fe^{54}$, $Fe^{58}-Ni^{58}$, and $Ni^{64}-Zn^{64}$, the packing fraction of larger atomic number elements is always larger algebraically than that of small atomic number elements. The dotted line in this figure shows the general tendency of the packing fraction curves in this region. It is seen from these curves that Dempster's packing fractions[5] in this region are slightly large, and that the minimum of our packing fraction curve is located about Cr or Fe, though in Dempster's curve it is located about Ti.

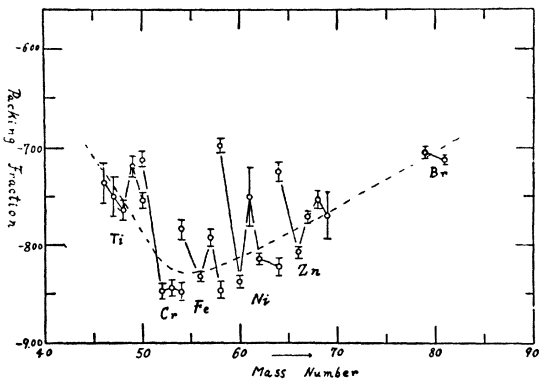

FIG. 1. Packing fraction curve in the region Ti to Br.

TABLE I.

Element	Z	A	Isotopic weight	Packing fraction	Binding energy (10^{-3} M.U.) Exp.	Theor.
Cr	2	50	49.96443± 3.9×10⁻⁴	−7.11±0.08	463.3	463
		52	51.95598± 4.4×10⁻⁴	−8.47±0.08	489.6	485
		53	52.95527± 4.4×10⁻⁴	−8.44±0.08	499.3	495
		54	53.95427± 4.8×10⁻⁴	−8.47±0.09	509.2	504
Fe	26	54	53.95774± 4.8×10⁻⁴	−7.83±0.09	504.1	500
		56	55.95340± 2.7×10⁻⁴	−8.32±0.05	526.4	522
		57	56.95485± 5.2×10⁻⁴	−7.92±0.09	533.9	532
		58	57.95091± 4.9×10⁻⁴	−8.46±0.09	546.7	542
Zn	30	64	63.95365± 6.6×10⁻⁴	−7.24±0.10	594.4	594
		66	65.94676± 4.2×10⁻⁴	−8.07±0.06	619.2	616
		67	66.94826± 3.8×10⁻⁴	−7.71±0.06	626.6	625
		68	67.94885± 6.5×10⁻⁴	−7.53±0.09	635.0	635
		70	69.9461 ±17 ×10⁻⁴	−7.69±0.24	655.4	652
Br	35	79	78.94438± 5.0×10⁻⁴	−7.04±0.06	733.8	735
		81	80.94228± 3.8×10⁻⁴	−7.12±0.05	753.8	752

[1] K. Ogata, Proc. Phys.-Math. Soc. (Japan) **22**, 486 (1940).
[2] Private communication.
[3] T. Okuda and K. Ogata, Proc. Phys.-Math. Soc. (Japan) **25**, 374 (1943).
[4] T. Okuda, K. Ogata, H. Kuroda, S. Shindo, and S. Shima, Phys. Rev. **59**, 104 (1941).
[5] A. J. Dempster, Phys. Rev. **53**, 64 (1938).

Cloud-Chamber Evidence of a Meson-Nucleus Interaction*

G. E. VALLEY, C. P. LEAVITT, AND J. A. VITALE

Physics Department and Laboratory for Nuclear Science and Engineering, Massachusetts Institute of Technology, Cambridge, Massachusetts

November 12, 1948

IN September 1948 we successfully operated a cloud chamber filled with argon to a pressure of 105 atmospheres (at 15°C) in a magnetic field of 8800 gauss, and at an altitude of 12,730 feet above sea level (by Summit Lake on Mt. Evans in Colorado). Stereoscopic pictures

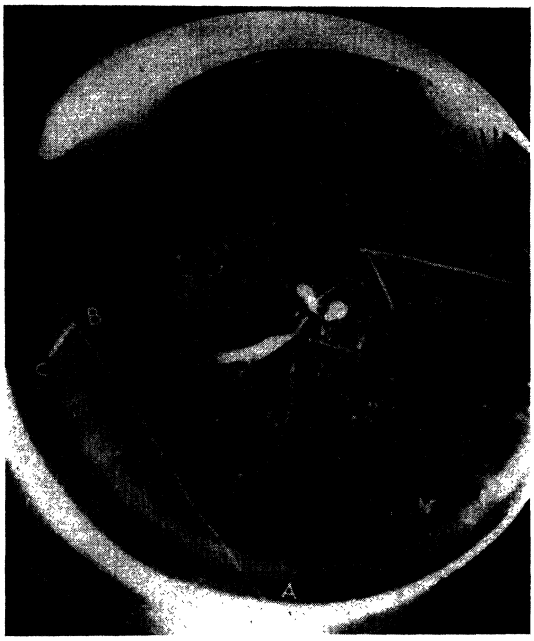

FIG. 1. High pressure cloud chamber picture showing a star produced by a non-ionizing particle, and a meson AB which produces a nucleon BC at the end of its path. The positive and negative ion tracks of the star are separated by the electric clearing field. The heavy plumes in the center of the picture are caused by corona from the clearing field electrode (6000 volts, 105 atmosphere argon, 8800 gauss, counter controlled).

were taken by means of two cameras, each inclined by 8° to the axis of symmetry.

The chamber was surrounded on top and sides by 11 cm of lead. During part of the experiment the instrument was triggered by hard showers produced by penetrating particles either in the lead or in the gas and walls of the chamber.

We observed the following phenomena:

(1) Production of positron-electron pairs in the gas.
(2) Particles apparently unaffected by the magnetic field which come to rest in the gas.
(3) Stars of one, two, three and four prongs produced in the gas by non-ionizing radiation. One of these is shown in Fig. 1.
(4) A comparatively high abundance of tracks similar to that marked ABC in Fig. 1. Here a long scattered track ends in a short straight section making a large angle with the original direction.

With counter control we observed five such tracks in 57 pictures. Without counter control we observed two such tracks in 135 pictures. Contrariwise the abundance of stars shows no dependence upon counter control at all. This is precisely what would be expected if the phenomena $A\ B\ C$ are locally produced and if the stars are produced by neutrons made in the atmosphere above. Locally produced neutrons are too few to have much probability of making a collision in the gas.

We have one picture which shows two such events in which the long components appear to emerge from a point just within the duralumin cloud-chamber wall. This we take to show that the particles which produce the long track proceed toward and not away from the juncture with the short track.

If it be assumed that the phenomenon represents the elastic or inelastic scattering of the particle which produced the long track, or that it represents the production of a single pronged star by virtue of the kinetic energy of that particle, then the total cross section for these processes is in excess of fifty barns. We calculate this by comparison of the abundance of these events with the abundance of tracks which stop in the gas and are also unaffected by the magnetic field.

Finally we have attempted in three cases to determine the mass of the "long" component by scattering-range measurements.

We set $\theta_1^2+\theta_2^2+\theta_3^2=\theta_4^2$ where θ_1 is the theoretical $R\ M\ S$ planar Coulomb scattering angle, θ_2 is the magnetic deflection angle over the same path and θ_3 is the "residual" or instrumental scattering of a very high energy track. The sum of the squares of these angles is then equal to the square of the angle actually measured, θ_4.

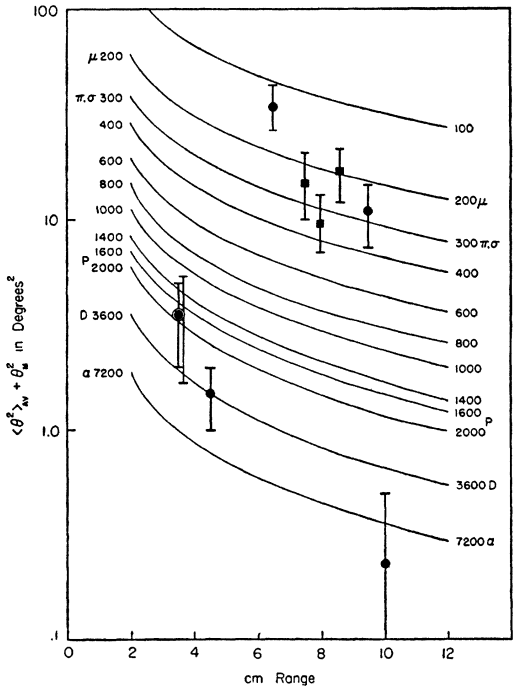

FIG. 2. Curves showing theoretical scattering plus magnetic deflection, for various masses over a range interval of 1 cm, against residual range in cm. Square points represent events like ABC in Fig. 1; round points represent heavily ionizing tracks which simply end in the gas.

In Fig. 2 we have plotted curves showing the sum $\theta_1^2+\theta_2^2$ *versus* range in cm under the conditions pertaining. We have superimposed, on this, points showing $\theta_4^2-\theta_3^2$ for several tracks. The square points are for the phenomena like $A\ B\ C$ of Fig. 1. The round points represent a random sample of heavy tracks which end in the gas. It is seen that these are well grouped into meson-like and nucleon-like particles and that in particular all of the phenomena like $A\ B\ C$ of Fig. 1 are mesons, whose precise mass we cannot here determine.

However, since these mesons are locally produced, they must be heavy, according to current ideas.

Unfortunately all our pictures of these events do not show so unequivocally that the short track is due to a nucleon or heavier particle. However, we have not observed any electrons to emerge from the ends of any of the short tracks.

We therefore conclude that these events show sigma-mesons which produce one-pronged stars, and for the present, put aside the less pleasant idea that μ-mesons rarely decay. Why we saw no π-μ-electron events remains to be investigated. It also must be investigated whether it is a property of argon alone, or of other of the lighter elements also, predominantly to boil off a single charged particle upon acceptance of a heavy meson.

We were ably and invaluably assisted in operating the heavy machinery by Thomas Mersereau. We are indebted to Professors B. B. Rossi and J. R. Zacharias for the advice and encouragement they gave us. We wish to express our appreciation to the many members of the staffs of M.I.T. and the Inter-University High-Altitude Laboratory, who helped us.

* This work was supported in part by the joint program of the Office of Naval Research and Atomic Energy Commission.

Temperature Dependence of Scintillations in Sodium Iodide Crystals

W. C. ELMORE
*Swarthmore College, Swarthmore, Pennsylvania**
AND
R. HOFSTADTER
*Princeton University, Princeton, New Jersey**
November 19, 1948

THE high speed "Microoscillograph"[1] and a new fast amplifier[2] have been employed in studying the temperature dependence of radium gamma-ray induced scintillations in thallium activated sodium iodide crystals.[3] In these studies light pulses were conducted by internal reflection along the length of a one-foot transparent fused quartz rod.[4] The crystal sample was placed, within a furnace, next to one polished end of the quartz rod. The photomultiplier was kept at room temperature and positioned at the other end of the quartz rod. After transformation of the light pulse to a current pulse, the photomultiplier signal was amplified approximately 200 times and brought to the plates of the Microoscillograph through short leads. Permanent records of the traces are obtained on the target photographic plates of the Microoscillograph. To obtain the records, a ten millicurie source was placed within a few inches of the crystals and random sweeps were used.

The polycrystalline NaI (Tl) samples were prepared by fusing in vacuum Baker and Adamson reagent grade sodium iodide together with 1 percent, by weight, of thallium iodide. The preparation is sealed off in a quartz tube in which the fusion takes place. Other samples were made containing 0.1 percent and 0.02 percent of Tl I.

At the present time the data allow only rough estimates to be made of the duration and pulse shape of the light emitted during a scintillation. This is due to the circumstance that the observed pulses do not show a unique shape or behavior. Some pulses, particularly the larger ones, rise as fast as the rise time of the amplifier ($\sim 2\times 10^{-8}$ sec.), while others build up to a maximum value over an interval of perhaps 0.1 microsecond. Still others show only an irregular structure. It is probable that the number of quanta, detected by the photomultiplier in the average scintillation, is not large enough to smooth statistically the pulse shape to a recognizable form. A distortion of the true pulse form also occurs in the larger pulses since they drive the amplifier into a non-linear region.

The results for duration of the light pulse are the following. At room temperature most pulses, whatever their shape, terminate in about 0.4 to 0.7 microsecond. At 150°C the pulses are over in about 0.3 to 0.4 microsecond. At 345°C the larger pulses decay to zero in approximately 0.15 microsecond. These results do not preclude the occurrence of single electron pulses following the main pulse by a time of the order of twice the given pulse duration.

We have also examined pulses obtained with the 0.1 percent and 0.02 percent Tl I samples and, for the same excitation, have observed fewer pulses than in the 1 percent sample but have noticed no change in the duration or shape of the individual pulses. We have also compared the total amount of light detected by the photomultiplier in a large scintillation at room temperature and at 345°C. At room temperature from three to five times as many quanta are detected per scintillation as in the corresponding case at the higher temperature. It is not known whether this result corresponds to a real decrease in the number of emitted quanta or to a shift in frequency of the emitted light band, although it is suspected that the former is the case.

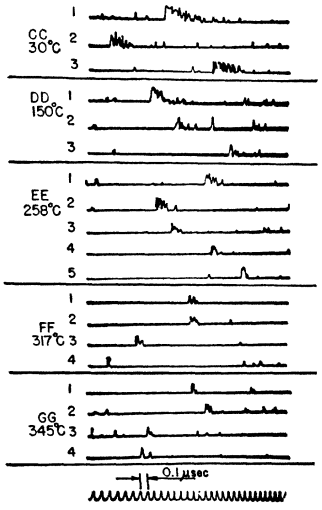

FIG. 1. Pulses showing sharp rise.

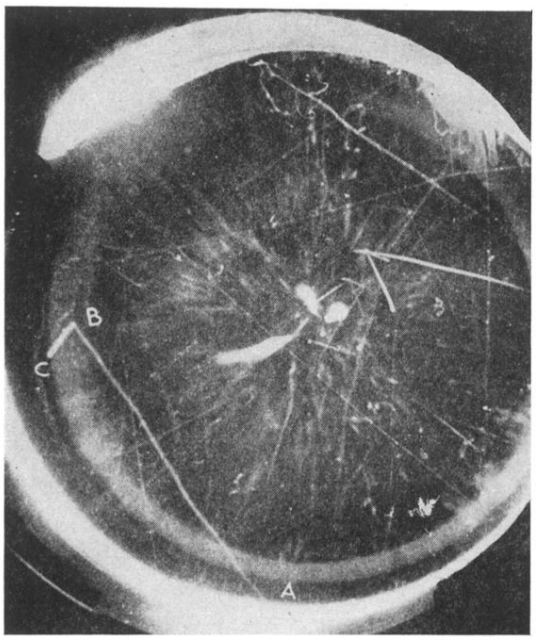

FIG. 1. High pressure cloud chamber picture showing a star produced by a non-ionizing particle, and a meson AB which produces a nucleon BC at the end of its path. The positive and negative ion tracks of the star are separated by the electric clearing field. The heavy plumes in the center of the picture are caused by corona from the clearing field electrode (6000 volts, 105 atmosphere argon, 8800 gauss, counter controlled).